Handbook on Emerging Trends in Scientific Research
ISBN: 978-969-9952-02-9
homepage: http://pakinsight.com
Conference venue: Nippon Hotel, İstanbul-Turkey
Vol.4 , 2015 (28,29 November)

Influence of Low Ag Doping on Structural, Morphological and Optical Properties of Sol-Gel Dip-coated Nanostructured ZnO Thin Films

M. Dehimi[1] --- T. Touam[2] --- A. Chelouche[3] --- F. Boudjouan[4] --- A. Bouasla[5] --- D. Djouadi[6] --- A. Fischer[7] --- A. Boudrioua[8] --- A. Doghmane[9]

[1,2,5,9]*Semiconductors Laboratory, University of Badji Mokhtar-Annaba, Algeria*
[3,4,6]*Environmental Engineering Laboratory, University of Bejaia, Bejaia, Algeria*
[7,8]*Laser Physics Laboratory CNRS UMR, University of Paris 13, Sorbonne Paris City, Villetaneuse, France*

Abstract

In the present study, a sol-gel dip-coating process was used to deposit almost stress free highly *c*-axis oriented nanostructured ZnO thin films on glass substrates. The effects of low silver doping concentration (Ag < 1 at.%) on the structural, morphological and optical properties of such films were investigated using different characterization techniques. X-ray diffraction (XRD) measurements have revealed that all the films were single phase and had a hexagonal wurtzite structure. The grain size values were calculated and found to be about 24-29 nm. Scanning electron microscopy (SEM) and atomic force microscopy (AFM) images have shown that film morphology and surface roughness were influenced by Ag doping concentration. Optical properties such as transmittance and optical bandgap energy (E_g) were examined using UV-Visible spectrophotometry. The results have indicated that all the prepared films were highly transparent with average visible transmission values ranging from 80% to 86%. Moreover, it was found that the Ag contents leads to widening of the bandgap.

Keywords: ZnO thin films, Low Ag doping, Sol–gel process, Structure and morphology, Optical properties.

Contribution/ Originality

This study is one of very few studies which have investigated the preparation of low Ag-doped ZnO thin films by the sol-gel dip-coating technique. It was put into evidence that incorporation of low Ag concentrations (Ag<1at.%) in ZnO can indeed improve its physical properties.

1. Introduction

In recent years, zinc oxide (ZnO) has emerged as a promising material for a large number of fundamental and applied fields due to its numerous interesting characteristics including direct wide band gap (3.37 eV) semiconductor with a large excitation binding energy (60 meV), material stability, high refractive indices, high values for second- and third-order nonlinear optical susceptibility tensors and high internal quantum well efficiency (Marotti *et al.*, 2006); (Qiu *et al.*, 2014); (Liu *et al.*, 2014); (Béaur *et al.*, 2011). These advantages place ZnO as an ideal candidate for several potential applications ranging from transparent conducting coatings (Chopra *et al.*, 1983) [5] to flat panel displays (Nam and Kwon, 2008) solar cell windows (Major and Chopra, 1988) photonic (Jia *et al.*, 2005) and surface acoustic wave devices (Peng *et al.*, 2013) as well as for the realization of new generation optoelectronic devices such as polariton lasers at room temperature (Zamfirescu *et al.*, 2002).

Undoped and doped ZnO thin films have been prepared by a variety of techniques such as spray pyrolysis (Karyaoui *et al.*, 2015) e-beam evaporation (Kim *et al.*, 2009) pulsed laser deposition (Wang *et al.*, 2011) chemical vapor deposition (Barnes *et al.*, 2005) direct current (DC) and radio frequency (RF) sputtering (Lee *et al.*, 2007); (Vasquez-A *et al.*, 2012) and sol gel methods (Xu *et al.*, 2005); (Xu *et al.*, 2015). Among these approaches, the sol–gel process has attracted large attentions due to its simplicity, low cost, easy adjusting composition and dopants, homogeneity on the molecular level and lower crystallization temperature.

ZnO doping with selective elements is the most effective alternative to improve its structural, electrical, magnetic, and optical properties without any change in the crystalline structure (Shin *et al.*, 2013); (Kim *et al.*, 2007). Among these elements, Ag has been one of the most extensively used dopants whose effects on ZnO thin film properties have been widely investigated (Xu *et al.*, 2005); (Xu *et al.*, 2015); (Gruzintsev *et al.*, 2003); (Kang *et al.*, 2006); (Liu *et al.*, 2010); (Jeong *et al.*, 2008); (Duan *et al.*, 2008); (Xue *et al.*, 2008); (Liu *et al.*, 2008); (Chen *et al.*, 2009); (Sahu, 2007); (Xian *et al.*, 2013); (Zhou *et al.*, 2011). It was reported that the properties of Ag doped ZnO thin films are strongly influenced by deposition techniques, fabrication parameters, annealing treatments and Ag doping concentrations. Despite this large number of experimental reports of Ag doped ZnO thin films, no consensus has been reached; the published data are mostly inconsistent and controversial (Xu *et al.*, 2005); (Xu *et al.*, 2015); (Gruzintsev *et al.*, 2003); (Kang *et al.*, 2006); (Liu *et al.*, 2010); (Xue *et al.*, 2008); (Liu *et al.*, 2008); (Chen *et al.*, 2009); (Sahu, 2007); (Xian *et al.*, 2013). Furthermore, only moderate or high Ag doping levels where studied. In this context, we complete and enrich our understanding of Ag doped ZnO films via the investigation of the influence of low Ag doping concentrations (Ag < 1 at.%) on ZnO thin films properties. In the present work, ZnO thin films have been deposited onto glass substrates using a sol-gel dip-coating process. A systematic study was conducted to reveal the effect of low silver doping concentration on the structural, morphological and optical properties by using various characterization techniques.

2. Experimental Details

Undoped and Ag doped ZnO thin films were prepared by the sol-gel process. As a starting material, zinc acetate dihydrate ($Zn(CH_3COO)_2$ $2H_2O$)(Sigma-Aldrich) was dissolved in a mixture of absolute ethanol (EtOH, 100%, BioChem) and monoethanolamine (MEA) (Sigma-Aldrich) yielding to a precursor concentration of 0.75 mol. L^{-1}. The MEA to zinc acetate molar ratio was set to 1. For doped films, silver nitrate ($AgNO_3$) was added to the mixture with an atomic percentage fixed at 0.3, 0.5, 0.7 and 0.9 at.% Ag, respectively. The resulting sols were magnetically stirred at 60 °C for 1 hour, and then aged at room temperature for two days to get clear and transparent homogeneous solutions. Prior to film deposition, commercial glass substrates (Esco Optics) were ultrasonically cleaned by using deionized water, ethanol and acetone for 15 min, respectively. Then, the substrates were dried in an oven at 100°C for 30 min. The substrates were dipped in the prepared sols and then withdrawn at a constant dip-coating speed of 15 mm/min (KSV 67 NIMA dip coater). After each deposition, all samples were preheated at 200 °C for 10 min to remove the solvent and organic residuals. This process cycle was repeated 6 times to increase the film thickness. These samples were annealed in an air atmosphere furnace for one hour at 500 °C and then cooled to room temperature before taken to the material characterization stage. The crystalline structure of ZnO thin films thus prepared was characterized via the XRD technique with a PanAlytical diffractometer. The latter was operated at 40 kV and 30 mA using Cu Kα radiation at a grazing incidence (ω = 0.54°). The micro-structures associated with the sol-gel derived ZnO films were analyzed by using the technique of SEM by a Raith PIONEER System. Surface morphology of thin films was examined in contact mode by a Nanosurf easy Scan 2 operated at room temperature and equipped with a 10 μm x 10 μm high resolution scanner with vertical range of 2 □m. AFM images have been recorded with a resolution of 512 x 512 pixels. The optical transmittance spectra were collected at room temperature by a Safas UVmc^2 UV–Vis spectrophotometer and the optical bandgap energy data was then derived from the transmission spectra.

3. Results and Discussion

The crystalline structure and orientation of all the prepared thin films were studied using XRD with their patterns recorded in a θ-2θ mode from 25 up to 70° at a resolution of 0.017° per step size. Displayed in figure 1(a) are the typical XRD spectra of samples associated with the conditions of undoped and Ag doped ZnO thin films at different concentrations. The angular peak position of the XRD signals corresponding to bulk ZnO is indicated by a dotted line located at 2θ = 34.43° (figure 1(b)) according to the XRD assignment by the American Society for Testing and Materials ASTM: 36-1451. It can clearly be seen from the XRD data that there are no extra peaks due to silver or any zinc silver phase, indicating that the synthesized films are in a single phase of hexagonal wurtzite structure. Moreover, the strong peak along [002] direction confirms that the ZnO is well crystallized and the crystallites are highly oriented with their c-axes normal to the deposition substrate plane. From figure 1(a) and 1(b), it can be seen that increasing the silver concentration does not affect the preferential growth of the films. In addition, the angular peak position value of (002) planes did not shift and almost perfectly match the angular value of ideal ZnO bulk peak demonstrating that the lattice parameter c almost did not change and was not influenced by the Ag doping levels in the starting solution.

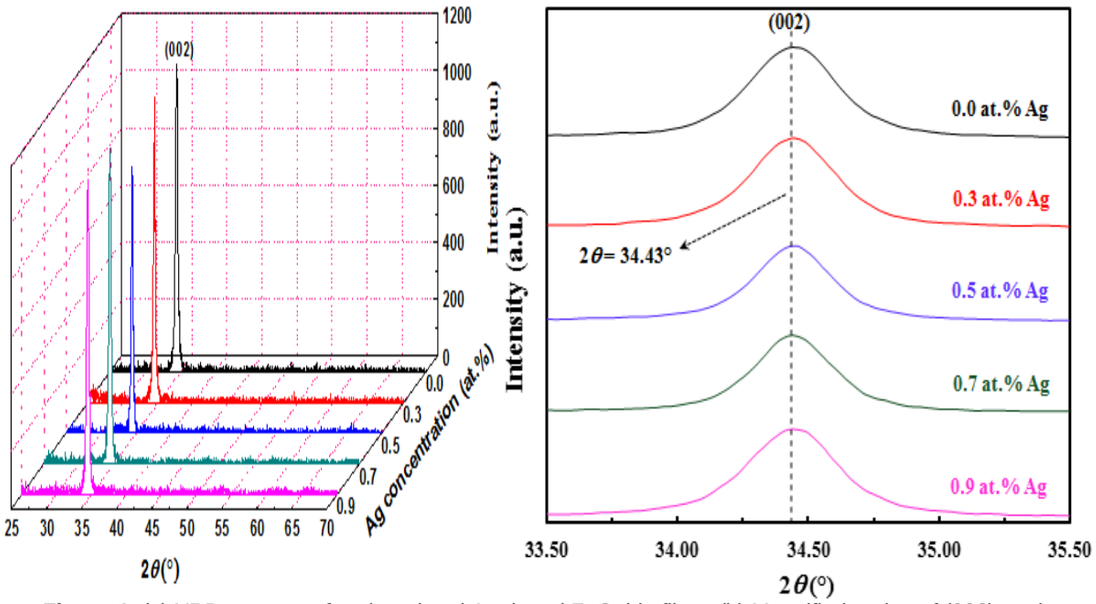

Figure-1. (a) XRD patterns of undoped and Ag doped ZnO thin films, (b) Magnified region of (002) peak.

The residual stress (σ) of the thin films can be determined from a biaxial strain model analysis (Puchert *et al.*, 1996). Accordingly, the lattice parameters and elastic stiffness constants of the single crystal ZnO are related in the following formula:

$$\sigma = \frac{2C_{13}^2 - C_{33}(C_{11}+C_{12})}{2C_{13}} X \frac{(c-c_0)}{c_0} \qquad (1)$$

Where c_0 = 5.206 Å is the unstrained lattice constant of ZnO along the *c*-axis and *c* is the lattice parameter of strained ZnO films calculated from the XRD data by means of the Bragg equation. C_{13} = 104,2 GPa, C_{33} = 213,8 GPa, C_{11} = 208,8 GPa and C_{12} = 119,7 GPa are the elastic stiffness constant values of single crystal ZnO (Chen *et al.*, 1996).

In figure 2 we illustrate the data of *c* lattice constant and residual stress converted from the above analysis for the undoped and Ag doped ZnO thin films. It can be noted that with increase of Ag doping concentration, the lattice parameter value was found to remain unchanged and equal to that of undoped ZnO. These observations show that undoped and Ag doped ZnO thin films deposited by our developed sol-gel process were virtually stress free and highly *c*-axis oriented.

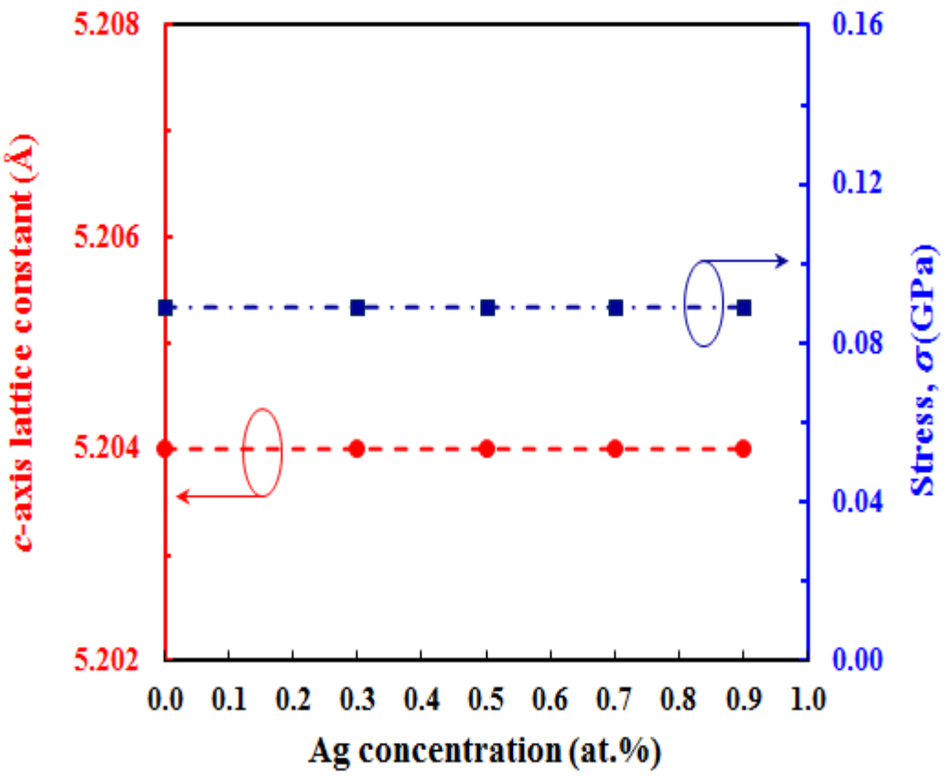

Figure-2. c-axis lattice constant and residual stress of undoped and Ag doped ZnO thin films

Concentrations, the full-width at half-maximum (FWHM) corresponding to the XRD (002) peaks was measured and depicted in figure 3. The average crystallite sizes, *D*, of these *c*-axis oriented thin films were estimated from the FWHM of (002) diffraction peak according to the well-known Scherer's formula (Langford and Wilson, 1978):

$$D = \frac{0.9\lambda}{\beta \cos\theta} \qquad (2)$$

Where λ = 0.154056 nm is the X-ray wavelength and β is the FWHM of the XRD signal with peak position at θ in radian.

Figure 3 illustrates the calculated average crystallite size values for undoped and Ag doped samples at different concentrations. The mean crystallite size is seen to be strongly dependent on the amount of Ag doping. As can be found in figure 3, the crystallite size is increased from 27.1 nm (Ag = 0.3 at.%) to a maximum value of 28.9 nm for the ZnO thin film doped at 0.5 at.%. However, opposite tendency is observed for higher Ag doping levels (> 0.5 at.%) i. e., the crystallite size is found to decrease with Ag concentration from 25.5 nm (Ag = 0.7 at.%) to 24.9 nm (Ag = 0.9 at.%). Such behavior of the crystallite size may be explained as follows: for Ag concentration less than or equal to 0.5 at.%, the Ag^{+} is probable to act as an amphoteric dopant and can occupy both the lattice and interstitial site. However, due to the difference of ionic charge and radius between Zn^{2+} ion (0.088 nm) and Ag^{+} ion (0.129 nm), the segregation of Ag at the vicinity of the grain boundary of ZnO is preferred which probably favors the preferential growth of larger sized crystallites associated with a slight decrease in the maximum intensities of the (002) diffraction peak. Whereas for Ag doping amounts higher than 0.5 at%, since the solubility of Ag in ZnO is low, Ag atoms are incorporated in the grain boundaries and/or into the film surface leading to a reduction in the crystal grain size. Similar trends have been observed in ZnO using Ag and other dopants (Kuo *et al.*, 2007); (Sanchez-Juarez *et al.*, 1998). The obtained results indicate that the addition of Ag may control the crystallite size of ZnO as observed for other transition metals such as Co and Cr (Volbers *et al.*, 2007); (Li *et al.*, 2009).

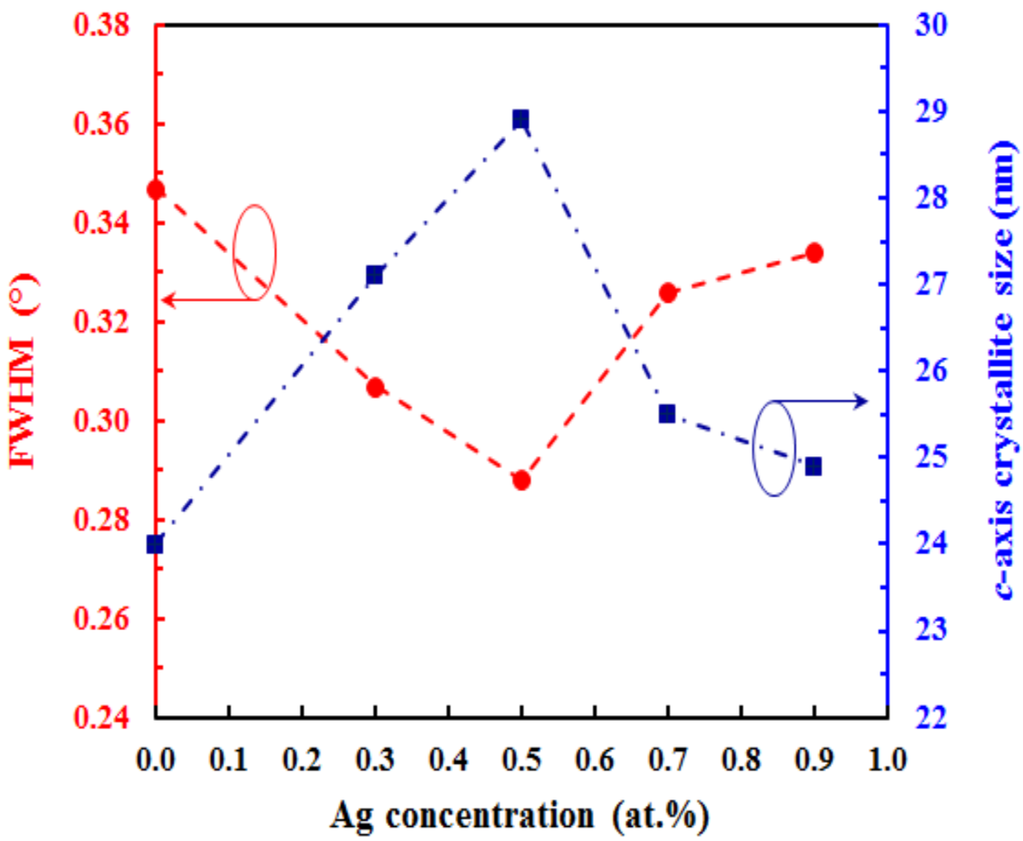

Figure-3. FWHM and c-axis lattice crystallite size of undoped and Ag doped ZnO thin films.

Undoped and Ag doped ZnO thin films were analyzed by SEM and AFM techniques in order to study their surface morphology and roughness. Prior to SEM imaging, the samples were coated with a 20 - 30 nm thick conducting layer of silver to prevent charge build-up. Figure 4 illustrates high-magnification SEM micrographs of the abovementioned samples. All the films showed a uniformly distributed like spherical shaped grains and compactly packed grains distributed over the film surface. It is clear from these micrographs that the surface morphology of the ZnO films seems to be influenced by the Ag doping. The undoped ZnO thin film exhibits a smooth surface consisting of small spherical grain size particles. Whereas, the surface morphology of the Ag doped ZnO thin films revealed different morphologies of the surface grains, which depend on Ag concentration. The average particle sizes increased with increasing percentage of Ag up to 0.5 at.%. Beyond this, the particle size exhibits reverse behavior and starts decreasing with increasing Ag doping levels. This trend in the average particle sizes observed by SEM is in good agreement with that of crystallite sizes obtained from XRD data analysis.

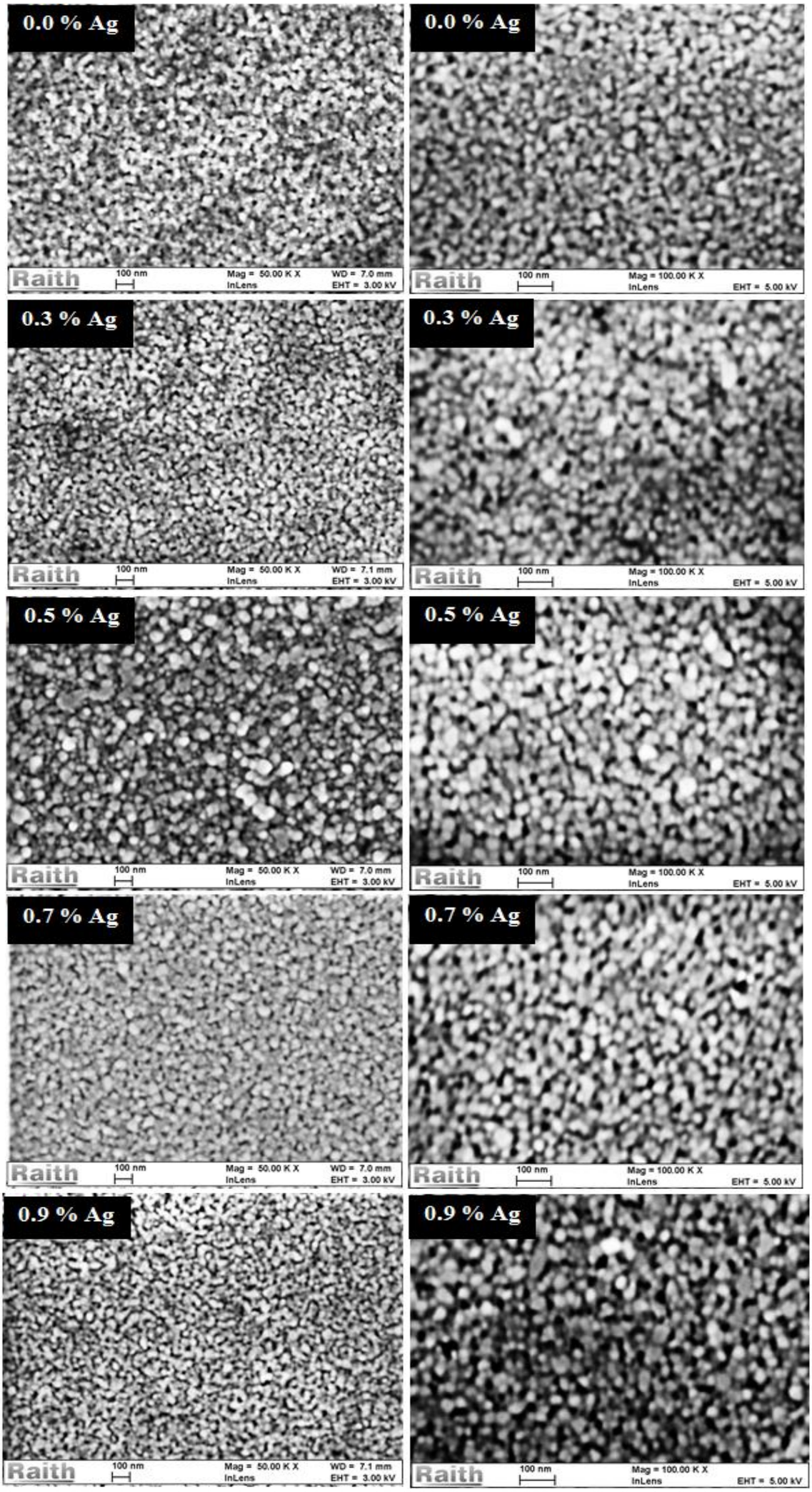

Figure-4. SEM micrographs of undoped and Ag doped ZnO thin films, x 50,000 magnification (on the left sides) and x 100,000 magnification (on the right sides).

Surface morphology of the thin films in terms of root mean squared roughness (R_{rms}) was explored from the AFM collected images using the Gwyddion analysis software (Nečas and Klapetek, 2012). The R_{rms} not only describes the light scattering but also gives an idea about the quality of the surface under investigation. Figure 5(a), 5(b), 5(c), 5(d) and 5(e) depict two-dimensional (2D) and three - dimensional (3D) AFM images of the undoped and Ag doped ZnO thin films with different concentrations scanned over a surface area of 1 × 1 μm^2.

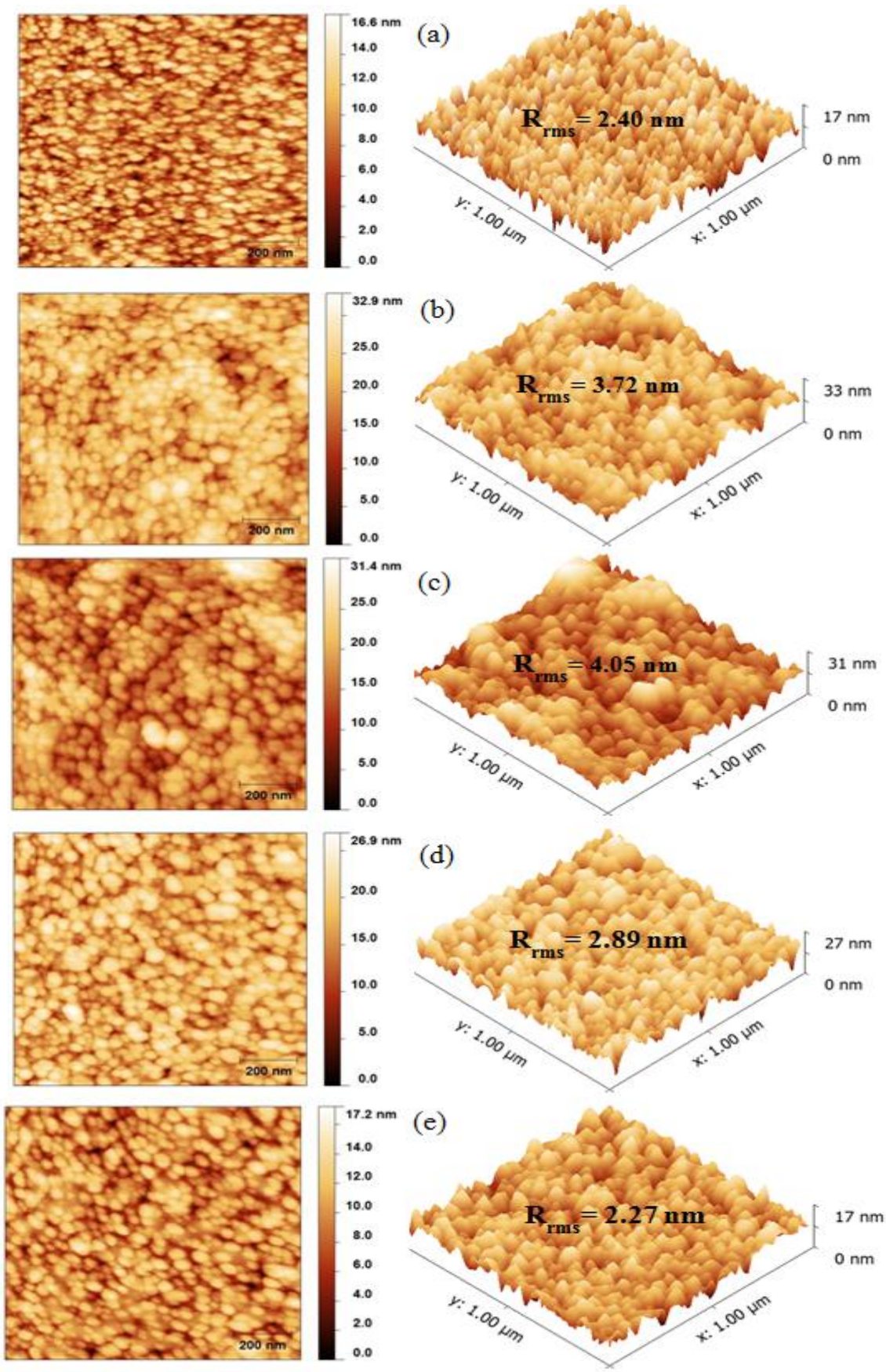

Figure-5. 2D and 3D AFM images of Ag doped ZnO thin films: (a) 0.0 at.% Ag, (b) 0.3 at.% Ag, (c) 0.5 at.% Ag, (d) 0.7 at.% Ag and (e) 0.9 at.% Ag.

It is clearly seen that the films exhibit different surface roughness which seems to be dependent on the Ag doping. From the data analyses, one can infer R_{rms} values of 2.40, 3.72, 4.05, 2.89 and 2.27 nm for undoped, 0.3, 0.5, 0.7 and 0.9 at.% Ag-doped ZnO thin films, respectively. It can be seen that the undoped ZnO thin film exhibits a low surface roughness.

However, increasing Ag doping levels leads to an increase in R_{rms} to reach a maximum value of 4.05 nm at 0.5 at.% Ag contents; it then gradually decreases down to a minimum value of 2.27 nm at 0.9 at.% Ag. According to this result, the enhancement in the surface roughness with the Ag content may be attributed, to the decrease of ZnO grain sizes as revealed by SEM micrographs. Furthermore, the Ag doping may reduce the scattering at the film surface as reported by previous works (Xue *et al.*, 2008); (Kuo *et al.*, 2007). Therefore, using Ag doped ZnO may improve the optical quality of the films, which are directly dependent on the roughness. Once again, the R_{rms} values exhibit a similar tendency to that of crystallite and grain sizes observed from XRD and SEM analysis.

Figure 6(a) shows the optical transmittance spectra of undoped and Ag doped ZnO thin films at different concentrations measured with respect to air in the 300–1000 nm range. It can clearly be seen that the films are highly transparent in the visible region with an average optical ranging from 80% to 86 %. A slight decrease in average transmittance from 81.3 % to 80 % was observed for undoped and Ag doped ZnO films at 0.5 at.%, respectively. However, for doping amounts higher than 0.5 at.% the films have shown better transparency with a maximum average transmittance value of about 86 % obtained at 0.9 at.% Ag concentration. These results may be attributed to the surface roughness trends revealed by AFM analysis, as it was put into evidence that 0.5 at.% doped films showed a maximum R_{rms} value whereas a minimum value was obtained for films with 0.9 at.% concentration.

The direct bandgap energies (E_g) of all the samples were determined by using a technique based on the derivative of the transmittance (T) with respect to energy (E), dT/dE, taking into account that ZnO is a direct band gap semiconductor. This accurate method has been used by several authors (Wang *et al.*, 2008). According to the measured transmission spectra, the dT/dE curves of undoped and Ag doped ZnO thin films at different concentrations are illustrated in figure 6(b). Our analysis indicates that the E_g of undoped ZnO film was found to be 3.229 eV in very good agreement with literature (Jun and Koh, 2012). Whereas the bandgap of Ag doped films increases initially then saturates at about 3.462 eV for all Ag doping concentrations. This widening of the optical band gap suggests that the Ag^+ was not substituted into the Zn^{2+} (Jeong *et al.*, 2007) and typically can be explained in term of Burstein-Moss shift (Burstein, 1954); (Moss, 1954).

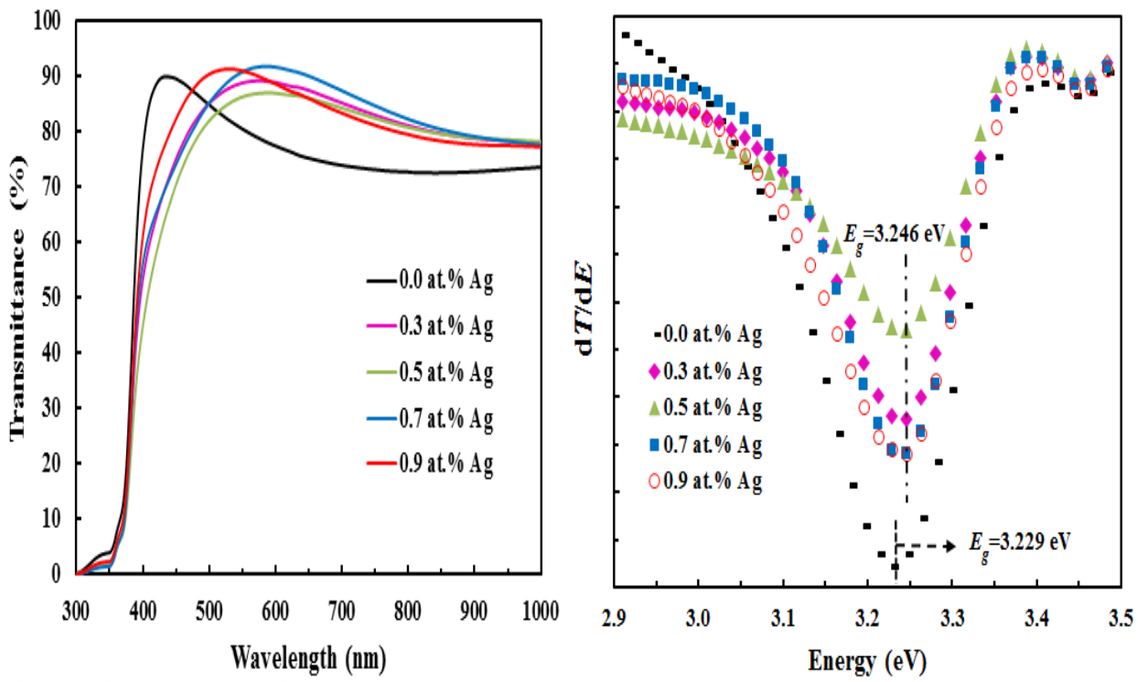

Figure-6. (a) UV–Vis transmittance spectra of undoped and Ag doped ZnO thin films, (b) dT/dE plots of undoped and Ag doped ZnO thin films.

4. Conclusion

Undoped and Ag doped ZnO thin films were successfully deposited onto glass substrates by the sol-gel dip-coating process. The effects of low silver doping concentration (Ag < 1 at.%) on the structural, morphological and optical properties were investigated. XRD measurement revealed that all films were single-phase hexagonal wurtzite structure, highly c-axis oriented and almost stress free. SEM micrographs and AFM images showed that film morphology and surface roughness were affected by low Ag doping concentration. All the films were highly transparent with average visible transmission values ranging from 80% to 86%. The Burstein-Moss effect was observed in all Ag doped ZnO thin films. Based on all the obtained results, it can be concluded that ZnO thin films doped with Ag concentrations as low as 0.7 and 0.9 at.% revealed interesting characteristics of enhanced crystalline quality, low surface roughness and high transparency suitable for photonic applications

References

Barnes, T.M., J. Leaf, C. Fry and C.A. Wolden, 2005. Room temperature chemical vapour deposition of c-axis ZnO. Journal of Crystal Growth, 274(3–4): 412–417.

Béaur, L., T. Bretagnon, B. Gil, A. Kavokin, T. Guillet, C. Brimont, D. Tainoff, M. Teisseire and J.M. Chauveau, 2011. Exciton radiative properties in nonpolar homoepitaxial ZnO/ (Zn,Mg) O quantum wells. Physical Review B, 84(16): 165312. DOI http://dx.doi.org/10.1103/PhysRevB.84.165311.

Burstein, E., 1954. Anomalous optical absorption limit in inSb. Physical Review, 93(3): 632–633.

Chen, M., Z.L. Pei, C. Sun, L.S. Wen and X. Wang, 1996. Surface characterization of transparent conductive oxide al-doped ZnO films. Journal of Crystal Growth, 220(3): 254–262.

Chen, Y., X.L. Xu, G.H. Zhang, H. Xue and S.Y. Ma, 2009. A comparative study of the microstructures and optical properties of Cu-and Ag-doped ZnO thin films. Physica B: Condensed Matter, 404(20): 3645–3649.

Chopra, K.L., S. Major and D.K. Pandya, 1983. Transparent conductors-a status review. Thin Solid Films, 102(1): 1–46.

Duan, L., W. Gao, R. Chen and Z. Fu, 2008. Influence of post-annealing conditions on properties of ZnO: Ag films. Solid State Communications, 145(9–10): 479–481.

Gruzintsev, A.N., V.T. Volkov and E.E. Yakimov, 2003. Photoelectric properties of ZnO films doped with Cu and Ag acceptor impurities. Semiconductors, 37(3): 259–262.

Jeong, E.K., I.S. Kim, D.H. Kim and S.Y. Choi, 2008. Effect of deposition and annealing temperature on structural, electrical and optical properties of Ag doped ZnO thin films. Korean Journal of Materials Research, 18(2): 84–91.

Jeong, S.H., B.N. Park, S.B. Lee and J.H. Bo, 2007. Metal-doped ZnO thin films: Synthesis and characterizations. Surface and Coatings Technology, 201(9–11): 5318–5322.

Jia, C.L., K.M. Wang, X.L. Wang, X.J. Zhang and F. Lu, 2005. Formation of c-axis oriented ZnO optical waveguides by radio-frequency magnetron sputtering. Optics Express, 13(13): 5093–5099.

Jun, M.C. and J.H. Koh, 2012. Effects of NIR annealing on the characteristics of al-doped ZnO thin films prepared by RF sputtering. Nanoscale Research Letters, 7: 294-297. DOI 10.1186/1556-276X-7-294.

Kang, H.S., B.D. Ahn, J.H. Kim, G.H. Kim, S.H. Lim, H.W. Chang and S.Y. Lee, 2006. Structural, electrical, and optical properties of p-type ZnO thin films with Ag dopant. Applied Physics Letters, 88(20): 202108-202113.

Karyaoui, M., A. Mhamdi, H. Kaouach, A. Labidi, A. Boukhachem, K. Boubaker, M. Amlouk and R. Chtourou, 2015. Some physical investigations on silver-doped ZnO sprayed thin films. Materials Science in Semiconductor Processing, 30: 255–262. DOI 10.1016/j.mssp.2014.09.017.

Kim, I.S., E.K. Jeong, D.Y. Kim, M. Kumar and S.Y. Choi, 2009. Investigation of p-type behavior in Ag-doped ZnO thin films by E-beam evaporation. Applied Surface Science, 55(7): 4011–4014.

Kim, K.C., E.K. Kim and Y.S. Kim, 2007. Growth and physical properties of sol–gel derived co doped ZnO thin film. Superlattices and Microstructures, 42(1-6): 246–250.

Kuo, S.T., W.H. Tuan, J. Shieh and S.F. Wang, 2007. Effect of Ag on the microstructure and electrical properties of ZnO. Journal of the European Ceramic Society, 27(16): 4521–4527.

Langford, J.I. and A.J.C. Wilson, 1978. Scherrer after sixty years: A survey and some new results in the determination of crystallite size. Journal of Applied Crystallography, 11(2): 102-113.

Lee, J.B., C.K. Park and J.S. Park, 2007. Physical properties of RF-sputtered ZnO thin films: Effects of two-step deposition. Journal of the Korean Physical Society, 50(4): 1073–1078.

Li, L., W. Wang, H. Liu, X. Liu, Q. Song and S. Ren, 2009. First principles calculations of electronic band structure and optical properties of Cr-doped ZnO. Journal of Physical Chemistry C, 113(9): 8460–8464.

Liu, K., B. Yang, H. Yan, Z. Fu, M. Wen, Y. Chen and J. Zuo, 2008. Strong room-temperature ultraviolet emission from nanocrystalline ZnO and ZnO: Ag films grown by ultrasonic spray pyrolysis. Applied Surface Science, 255(7): 2052–2056.

Liu, M., S.W. Qu, W.W. Yu, S.Y. Bao, C.Y. Ma, Q.Y. Zhang, J. He, J.C. Jiang, E.I. Meletis and C.L. Chen, 2010. Photoluminescence and extinction enhancement from ZnO films embedded with Ag nanoparticles. Applied Physics Letters, 97(23): 231906.

Liu, W., K. Wang, H. Long, S. Chu, B. Wang and P. Lu, 2014. Near-resonant second-order nonlinear susceptibility in c-axis oriented ZnO nanorods. Applied Physics Letters, 105(7): 071906.

Major, S. and K.L. Chopra, 1988. Indium-doped zinc oxide films transparent electrodes for solar cells. Solar Energy Materials and Solar Cells, 17(5): 319–327.

Marotti, R.E., P. Giorgi, G. Machado and E.A. Dalchiele, 2006. Crystallite size dependence of band gap energy for electrodeposited ZnO grown at different temperatures. Solar Energy Materials and Solar Cells, 90(20): 2356–2361.

Moss, T.S., 1954. The interpretation of the properties of indium antimonide. Proceedings of the Physical Society of London B, 67(10): 775–782.

Nam, G.M. and M.S. Kwon, 2008. Transparent conducting Ga-doped ZnO thin films for flat-panel displays with a sol-gel spin coating. Journal of Information Display, 9(1): 8–11.

Nečas, D. and P. Klapetek, 2012. Gwyddion: An open-source software for SPM data analysis. Central European Journal of Physics, 10(1): 181–188.

Peng, W., Y. He, X. Zhao, H. Liu, X. Kang and C. Wen, 2013. Study on the performance of ZnO nanomaterial-based surface acoustic wave ultraviolet detectors. Journal of Micromechanics and Microengineering, 23(12): 125008.

Puchert, M.K., P.Y. Timbrell and R.N. Lamb, 1996. Postdeposition annealing of radio frequency magnetron sputtered ZnO films. Journal of Vacuum Science & Technology A, 14(4): 2220–2230.

Qiu, K., Y. Zhao, Y. Gao, X. Liu, X. Ji, S. Cao, J. Tang, Y. Sun, D. Zhang, B. Feng and X. Xu, 2014. Refractive index of a single ZnO microwire at high temperatures. Applied Physics Letters, 104(1): 081109. DOI http://dx.doi.org/10.1063/1.4866668.

Sahu, D.R., 2007. Studies on the properties of sputter-deposited Ag-doped ZnO films. Microelectronics Journal, 38(12): 1252–1256.

Sanchez-Juarez, A., A. Tiburcio-Silver, A. Ortiz, E.P. Zironi and J. Rickards, 1998. Electrical and optical properties of fluorine-doped ZnO thin films prepared by spray pyrolysis. Thin Solid Films, 333(1–2): 196–202.

Shin, S.W., I.Y. Kim, K.S. Jeon, J.Y. Heo, G.S. Heo, P.S. Patil, J.H. Kim and J.Y. Lee, 2013. Wide band gap characteristic of quaternary and flexible Mg and Ga co-doped ZnO transparent conductive thin films. Journal of Asian Ceramic Societies, 1(3): 262–266.

Vasquez-A, M.A., O. Goiz, R. Baca-Arroyo, J.A. Andraca-Adame, G. Romero-Paredes and R. Peña-Sierra, 2012. Study of the properties of ZnO: Zn thin films obtained from ZnO/Zn/ZnO structure deposited by DC sputtering. Journal of Nanoscience and Nanotechnology, 12(12): 9234–9237.

Volbers, N., H. Zhou, C. Knies, D. Pfisterer, J. Sann, D.M. Hofmann and B.K. Meyer, 2007. Synthesis and characterization of ZnO:Co2+ nanoparticles. Applied Physics A, 88(1): 153–155.

Wang, L.N., L.Z. Hu, H.Q. Zhang, Y. Qiu, Y. Lang, G.Q. Liu, J.Y. Ji, J.X. Ma and Z.W. Zhao, 2011. Studying the Raman spectra of Ag doped ZnO films grown by PLD. Materials Science in Semiconductor Processing, 14(3–4): 274–277.

Wang, M., E.J. Kim, S. Kim, J.S. Chung, I. Yoo, E.W. Hahn, S.H. Shin and C. Park, 2008. Optical and structural properties of sol–gel prepared Mg ZnO alloy thin films. Thin Solid Films, 516(6): 1124–1129.

Xian, F., K. Miao, X. Bai, Y. Ji, F. Chen and X. Li, 2013. Characteraction of Ag-doped ZnO thin film synthesized by sol-gel method and its using in thin film solar cells. Optik - International Journal for Light and Electron Optics, 124(21): 4876– 4879.

Xu, J., Z.Y. Zhang, Y. Zhang, B.X. Lin and Z.X. Fu, 2005. Effect of Ag doping on optical and electrical properties of ZnO thin films. Chinese Physics Letters, 22(8): 2031–2034.

Xu, L., G. Zheng, L. Zhao and S. Pei, 2015. Two different mechanisms on UV emission enhancement in Ag-doped ZnO thin films. Journal of Luminescence, 158: 396–400. DOI 10.1016/j.jlumin.2014.10.028.

Xue, H., X.L. Xu, Y. Chen, G.H. Zhang and S.Y. Ma, 2008. Influence of Ag-doping on the optical properties of ZnO films. Applied Surface Science, 255(5): 1806–1810.

Zamfirescu, M., A. Kavokin, B. Gil, G. Malpuech and M. Kaliteevski, 2002. ZnO as a material mostly adapted for the realization of room temperature polariton lasers. Physical Review B, 65(16): 161205.

Zhou, X.D., X.H. Xiao, J.X. Xu, G.X. Cai, F. Ren and C.Z. Jiang, 2011. Mechanism of the enhancement and quenching of ZnO photoluminescence by ZnO-Ag coupling. Europhysics Letter, 93(5): 57009.